Thermally Enhancing the Surface Areas of Yamamoto-Derived Porous Organic Polymers

Brad G. Hauser,[†,‡] Omar K. Farha,*,[†,‡] Jason Exley,[§] and Joseph T. Hupp*,[†]

[†]Department of Chemistry, Northwestern University, 2145 Sheridan Road, Evanston, Illinois 60208, United States
[§]Micromeritics Instrument Corporation, One Micromeritics Drive, Norcross, Georgia 30093, United States

S *Supporting Information*

ABSTRACT: Thermal treatment of highly stable porous organic polymers based upon the Yamamoto polymerization of 2,2′,7,7′-spirobifluorene was done. The polymers are shown to be thermally and chemically stable. Upon thermal treatment the polymers are shown to have BET surface areas of ca. 2,000 m²/g and 2,500 m²/g respectively.

KEYWORDS: *porous polymers, gas storage, polymer processing*
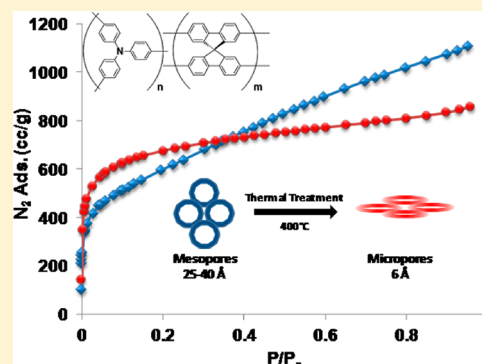
1. INTRODUCTION

New classes of high surface area microporous materials have recently garnered much attention for their possible use in heterogeneous catalysis,[1] gas storage,[2] and chemical separation[3] applications. Metal-ion-containing materials such as zeolites[4] and metal−organic frameworks (MOFs)[5] have been widely explored, as have nonmetallic materials such as covalent-organic frameworks (COFs),[6] polymers of intrinsic microporosity (PIMs),[7] porous organic polymers (POPs)[8] and others. Each of the aforementioned classes of materials possess inherent strengths and weaknesses. Because POPs and PIMs are composed almost exclusively of strong carbon−carbon, carbon−nitrogen, and/or carbon−oxygen bonds they possess chemical stability not normally evidenced in either COFs or MOFs.[9] In addition to high stability, POPs and PIMs have been synthesized with high accessible surface areas and allow for incorporation of a wide range of chemical functionality not possible in zeolites. However, due to the irreversible nature of the polymer growth, POPs are amorphous materials making characterization via X-ray crystallographic techniques all but impossible. Additionally, POPs are often highly catenated, thereby lowering the accessible surface area.[10]

Herein, we report on a new Yamamoto derived spriobifluorene network (YSN) and a method of thermal treatment to improve the overall gas adsorption of this highly stable form of POP. YSNs are based upon the Yamamoto polymerization of 2,2′,7,7′-tetrabromo-9,9′-spirobifluorene using *bis*-(1,5-cyclooctadiene)nickel(0) (Ni(COD)₂) as a catalyst. Spiro based monomers are common in the synthesis of polymers, and the distorted tetrahedral configuration of the center carbon

is exploited to induce porosity.[11] Schmidt et al. described the first YSN. They used the Yamamoto-Ullman coupling polymerization technique to form a microporous polymer.[12] Yamamoto polymerization was later used to form the "porous aromatic framework" PAF-1,[13] and the "porous polymer network" PPN-4;[14] these possess some of the highest BET surface areas of any materials yet reported: 5,600 m²/g and 6,460 m²/g respectively.

2. EXPERIMENTAL SECTION

2.1. Synthesis of YSNs. YSN-1: In an argon atmosphere glovebox 1.1 g of (Ni(COD)₂) (4.1 mmol, Strem Chemicals), 0.65 g of 2,2′-bipyridine (4.1 mmol), and 0.5 mL of 1,5-cyclooctadiene (4.1 mmol) were combined in a 100 mL round-bottom flask and dissolved in 60 mL of dry N,N′-dimethylformamide (DMF) with magnetic stirring. In a separate 15 mL round-bottom flask 0.5 g of 2,2′,7,7′-tetrabromo-9,9′-spirobifluorene monomer (0.79 mmol, Ark Pharm, Inc.) was added. The two flasks were joined by a 75° bent adapter. The joints were lightly greased to ensure airtight seals. The apparatus was taken out of the argon atmosphere glovebox, and the catalyst mixture was heated and stirred at 85 °C in a silicone oil bath for 2 h. The monomer was then added to the catalyst solution by carefully tilting the reaction apparatus. The reaction was stirred and heated at 85 °C for 16 h. The reaction was cooled to room temperature, and concentrated hydrochloric acid (approximately 10 mL) was added dropwise to the mixture until a yellow precipitate formed. The precipitate was isolated by filtration and rinsed with DMF (3 × 25 mL), water (3 × 25 mL), and acetone (3 × 20 mL) to remove any residual catalyst and

unreacted monomer. Solvent was removed by heating the material at 150 °C for 24 h under vacuum. A yield of 0.19 g (80%) was achieved.

YSN-2: In an argon atmosphere glovebox 2.7 g of (Ni(COD)₂) (9.7 mmol, Strem Chemicals), 1.6 g of 2,2′-bipyridine (10.1 mmol), and 0.5 mL of 1,5-cyclooctadiene (10.1 mmol) were combined in a 250 mL round-bottom flask and dissolved in 100 mL of dry DMF with magnetic stirring. 2,2′,7,7′-Tetrabromo-9,9′-spirobisfluorene (0.78 g, 1.2 mmol) and *tris*-(4-bromophenyl)amine (0.75 g, 1.6 mmol) were combined in a separate 15 mL round-bottom flask. By following the procedure above for the synthesis of **YSN-1**, the desired material, **YSN-2**, was isolated as a pale brown solid in 97% yield (0.735 g).

2.2. Thermogravimetric Analysis (TGA). All TGA was carried out on a Mettler-Toledo TGA/SDTA851e. Samples (4−6 mg) were loaded into a 70 μL alumina pan and heated to 1000 °C at a rate of 10 °C. Experiments were conducted under flow of ultra high purity grade nitrogen and compressed air.

2.3. Thermal Treatment of YSNs. For thermal treatment at temperatures of 400 °C or below, each YSN sample (20 mg) was loaded into a preweighed glass sample tube, placed in a Micromeritics Flow-Prep apparatus, and heated at the prescribed temperature overnight under a flow of ultra high purity nitrogen. The sample was allowed to cool to room temperature and then immediately subjected to gas adsorption analysis.

Thermal treatments at temperatures over 400 °C could not be done on the Flow-Prep due to instrument constraints. Consequently, samples were instead heated in a thermogravimetric analysis instrument (Mettler-Toledo TGA/SDTA851e). Approximately 15 mg of YSN was split between three 70 μL alumina pans and heated to the prescribed temperature at 15 °C/min and held for 1 h. The heated sample was then transferred into a preweighed glass sample tube and used for gas isotherm analysis after being placed under dynamic vacuum at room temperature for one hour.

2.4. Gas Sorption Measurements. Degassed samples were placed in a preweighed glass sample holder for gas isotherm analysis on a TriStar 3020 (Micromeritics Instruments). Nitrogen and hydrogen isotherms were held at a constant 77 K in a liquid nitrogen bath and 87 K in a liquid argon bath. Ultra high purity grade gases were used for analysis without further purification (Airgas Inc.). Surface areas were determined using BET theory using the previously described method.[15] Pore size distributions were calculated using the DFT method for nitrogen at 77 K on carbon with slit pore geometry (TriStar II 3020 software version 1.03). Micropore surface areas were calculated using the t-plot method assuming the Harking-Jura statistical thickness.

3. RESULTS AND DISCUSSION

The porosity of YSNs stems from the rigid architecture of the spirobifluorene monomer; no pore templating agents are used. Several POP syntheses, beginning with **YSN-1**, have taken advantage of this building unit.[16] Its synthesis, first described by Thomas and co-workers,[12] was aided by microwave heating and was accomplished using THF as solvent. Good yields were obtained (60−85%), and gas isotherm analysis showed the material to have a BET surface area of 1,280 m²/g. For the present study, a slightly modified synthetic procedure was used. The solvent, THF, was changed in favor of N,N′-dimethylformamide (DMF). A recent study suggests porous polymers formed in DMF tend to show higher surface area and microporosity than polymers synthesized in THF.[17] Additionally the reaction was run at 85 °C in an oil bath to slow the reaction and diminish catenation. These modifications afforded a polymer (**YSN-1**) with a BET surface area of 1,970 m²/g (see Table 1). Under similar conditions a new polymer (**YSN-2**) was synthesized by combining tetrabromo-spirobisfluorene monomer with *tris*-(4- bromophenyl)amine monomer (see Scheme 1). We anticipated good thermal stability for **YSN-1** and **YSN-2** as they are constructed of only strong covalent

Table 1. BET Surface Area (SA_BET) and Total Pore Volume (V_pore)

sample	SA_{BET} (m²/g)	$V_{pore}{}^b$ (cm³/g)
YSN[a]	1280	1.00
YSN-1	1970	1.20
YSN-1_400 °C	2510	1.00
YSN-1_500 °C	1400	1.50
YSN-1_600 °C	1530	1.60
YSN-2	1710	1.50
YSN-2_250 °C	1880	1.45
YSN-2_300 °C	2010	1.20
YSN-2_400 °C	1510	0.75

[a]Reference 12. [b]Total pore volume from DFT.

Scheme 1. Syntheses of YSN-1 (Top) and YSN-2 (Bottom)
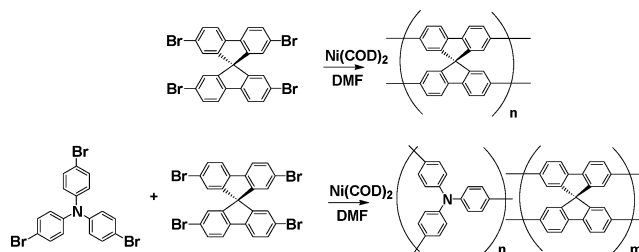
carbon−carbon and carbon−nitrogen bonds. To test the notion, thermogravimetric analyses (TGA) were performed; see Figure 1. Under flowing N₂, **YSN-1** displayed a ca. 5% mass
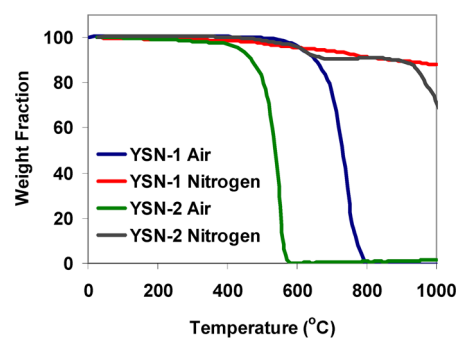

Figure 1. Thermogravimetric analysis traces of **YSN-1** under flow of nitrogen (red) and air (blue) and **YSN-2** under flow of nitrogen (black) and air (green).

loss near 600 °C and a second loss beginning around 800 °C. For **YSN-2**, substantial mass loss occurs only above ∼950 °C. For **YSN-1**, even at 1,000 °C (the upper limit of our instrument) less than 15% of the original mass is lost. Under flowing air, **YSN-1** pyrolyzes near 600 °C. By comparison, **YSN-2**, which contains comparatively weak carbon−nitrogen bonds, pyrolyzes at ca. 450 °C.

From the perspective of applications, a more useful measure of thermal stability is the persistence of porosity, as gauged by surface-area measurements. With this in mind, samples of **YSN-1** were heated to 400 °C, 500 °C, or 600 °C (**YSN-1**_400 °C, **YSN-1**_500 °C, and **YSN-1**_600 °C), and samples of **YSN-2** were heated to 250 °C, 300 °C, or 400 °C (**YSN-2**_250 °C, **YSN-2**_300 °C, and **YSN-2**_400 °C). Shown in Figure 2 are N₂ sorption isotherms. Remarkably, pretreatment at 400 °C increases the BET surface area of **YSN-1** by more than 500 m²/g relative to its initial value. (SA for **YSN-1**_400 °C = 2,510 m²/g.) Processing at higher
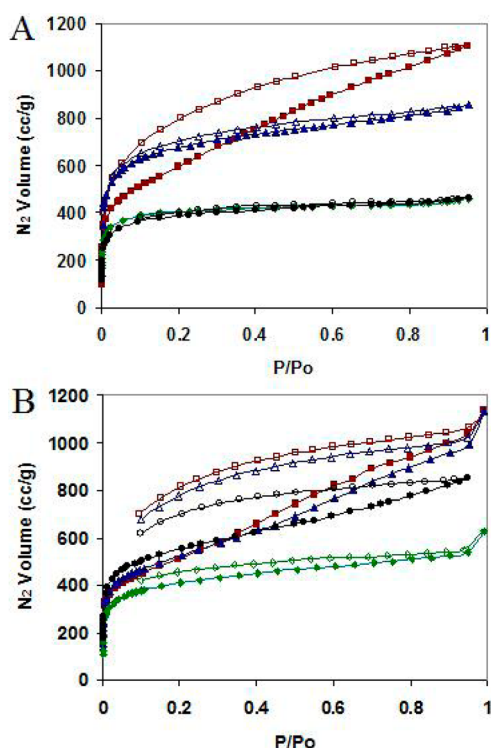
Figure 2. Nitrogen isotherm data for thermally treated a) **YSN-1** (**YSN-1** red; **YSN-1**$_{400 \,°C}$ blue; **YSN-1**$_{500 \,°C}$ black; **YSN-1**$_{600 \,°C}$ green) and b) **YSN-2** (**YSN-2** red; **YSN-2**$_{250 \,°C}$ blue; **YSN-2**$_{300 \,°C}$ black; **YSN-1**$_{400 \,°C}$ green). Closed symbols are for adsorption, open symbols are for desorption.

Figure 3. NLDFT pore size distributions of **YSN-1** (A) and **YSN-1**$_{400°C}$ (B).

temperature, however, decreases the surface area, with values for **YSN-1**$_{500 \,°C}$ and **YSN-1**$_{600 \,°C}$ equaling 1,410 m^2/g and 1,530 m^2/g, respectively. For **YSN-2**, heating at 300 °C increases the surface area by ca. 300 m^2/g (to 2,010 m^2/g), while heating to 400 °C engenders a 200 m^2/g decrease. Heating at 250 °C only gives a moderate increase to 1880 m^2/g.

Insights into the changes in surface area are provided by the shapes of the various nitrogen isotherms. In the absence of high-temperature processing (400 °C or greater), isotherms for both **YSN-1** and **YSN-2** display significant hysteresis − possibly indicative of mesoporosity. (If the hysteresis were solely due to mesoporsity, desorption/adsorption isotherm convergence below P/P$_0$ = 0.4 would be expected; instead convergence is absent.) An alternate or additional explanation for the hysteretic behavior is "plasticization and distension of the polymer and/or the twisted microporous network".[7b]

Independent evidence for the presence of mesopores comes from NLDFT analysis of isotherms at low pressures to obtain pore-size distributions. Figure 3, for example, shows that **YSN-1** contains a range of mesopores, with the distribution maximizing around 35 Å. In contrast, **YSN-1**$_{400 \,°C}$ features comparatively few mesopores. An initially attractive explanation was that **YSN-1** perhaps contained a significant quantity of unreacted terminal bromine atoms and that these were lost, with concomitant C−C bond formation upon heating to 400 °C. Further experiments, however, ruled this notion out. Specifically, elemental analyses of **YSN-1** and **YSN-1**$_{400 \,°C}$ showed no remaining bromine in either version of the polymer. Regardless of mechanism, observed losses of pore volume and increases in micropore surface area (Table 1) are consistent with compression of mesopores to micropores. If, in addition,
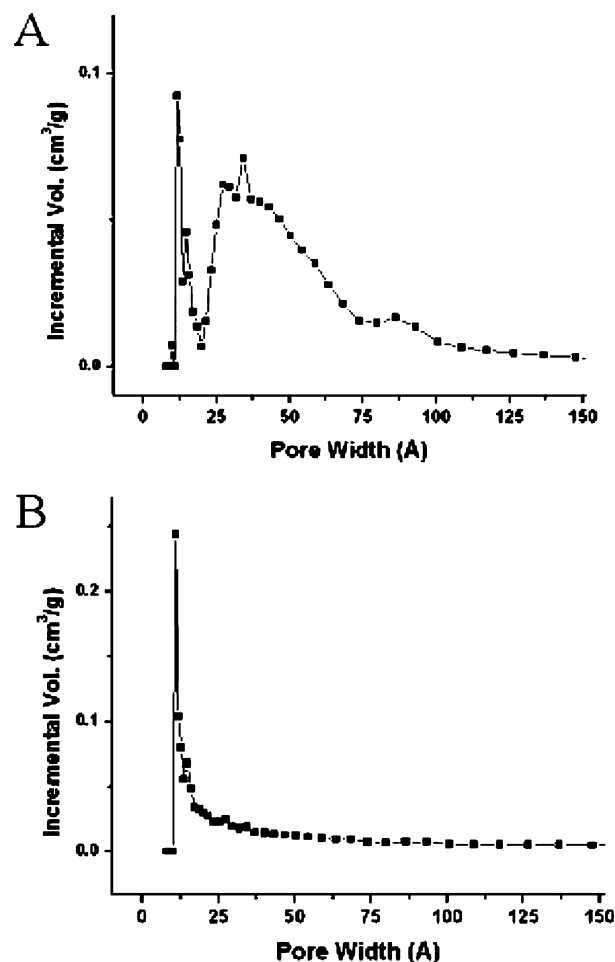
cross-linking is somehow engendered, this could well account for the observed enhancements of surface area following thermal processing.

The apparent chemical stabilities of **YSN-1** and **YSN-2** were also assessed. Polymer samples were placed in aqueous solutions of 1 M hydrochloric acid or 1 M potassium hydroxide and stirred at 85 °C for 24 h. The samples were isolated via filtration and rinsed with DI water. Prior to gas isotherm analysis the samples were heated under vacuum at 150 °C for 24 h to remove all solvent. Nitrogen isotherms were then collected and BET areas calculated. **YSN-1**$_{KOH}$ showed essentially no difference in surface area (SA = 1,970 m^2/g) versus the original material, while **YSN-1**$_{HCl}$ showed a marginal decrease (SA = 1,830 m^2/g). **YSN-2** likewise displayed little change in surface area following exposure to aqueous acid or base. (SA for **YSN-2**$_{HCl}$ = 1,580 m^2/g; SA for **YSN-2**$_{KOH}$ = 1,500 m^2/g.) In all cases, the YSN powder floated on the aqueous solutions and agitation produced a suspension. These observations suggest that the polymers are highly hydrophobic and, therefore, immune to permeation by aqueous solutions.

While our primary goal was to find routes to surface-area enhancement, we have briefly examined a potential application: cryogenic storage of molecular hydrogen. Much smaller isosteric heats of adsorption (q$_{st}$) are needed for storage at 77 K than at ambient temperature (i.e., a few to several kJ/mol versus ca. 20 kJ/mol). Hydrogen isotherms of **YSN-1** are given in Figure 4. At 77 K and 1 bar the uptake for **YSN-1** is 1.9 wt %.
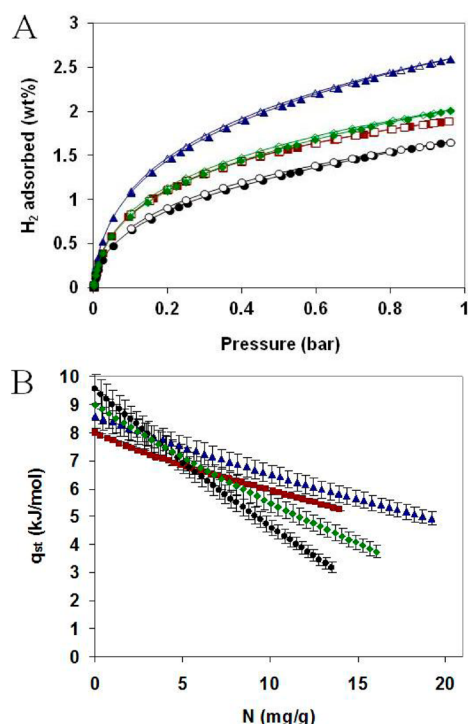
Figure 4. Hydrogen isotherm at 77 K (A) and isosteric heats of adsorption (B) of **YSN-1** (squares), **YSN-1$_{400 °C}$** (triangles), **YSN-1$_{500°C}$** (circles), and **YSN-1$_{600°C}$** (diamonds). Closed symbols adsorption; open symbols desorption.

The high temperature treated **YSN-1$_{400 °C}$** gives a 2.6 wt% hydrogen uptake at 1 bar nearly a 30% increase over **YSN-1**. Using data from isotherms measured at 77 K and 87 K the isosteric heats of adorption are calculated and given in Figure 5.
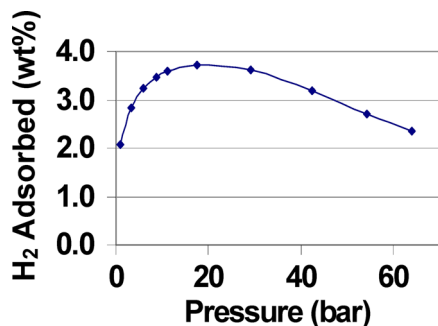

Figure 5. High-pressure hydrogen isotherm of **YSN-1** at 77 K.

The isosteric heat of adsorption (q_{st}) at zero loading for **YSN-1** is 8.0 kJ/mol. For **YSN-1$_{400 °C}$** the q_{st} is 0.5 kJ/mol higher than **YSN-1** and remains about 0.5 kJ/mol higher than the q_{st} for **YSN-1** through the entire loading regime. **YSN-2** also shows good uptake of hydrogen at 77 K and 1 bar (1.7 wt %). Thermal treatment of **YSN-2** at 250 and 300 °C increases the hydrogen uptake to 1.8 wt % and 2.3 wt % respectively (Figure 6). The increase in hydrogen uptake is reflected in the isosteric heats of adsorption with **YSN-2$_{250 °C}$** showing a nearly 1 kJ/mol increase in q_{st} over the entire range of H$_2$ loading. **YSN-2$_{300°C}$** has a q_{st} that, after a slight drop, remains level with increased loading. High-pressure adsorption by **YSN-1** was also measured at 77 K. The isotherm (Figure 5) shows a maximum excess uptake at 17 bar of 3.7 wt %.
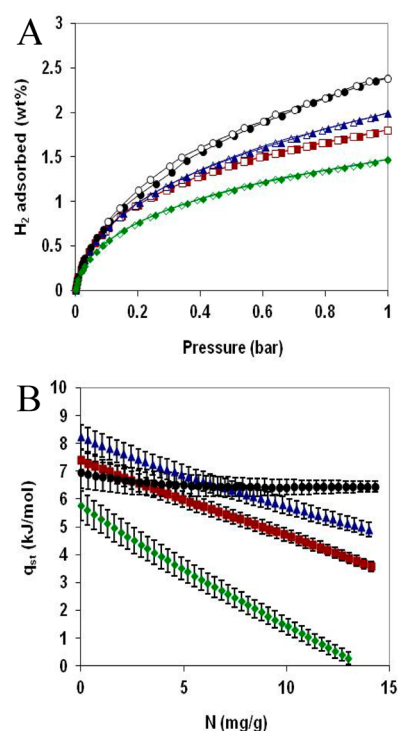

Figure 6. Hydrogen isotherms at 77 K (A) and isosteric heats of adsorption (B) of **YSN-2** (squares), **YSN-2$_{250°C}$** (triangles), **YSN-2$_{300°C}$** (circles), and **YSN-2$_{400°C}$** (diamonds). Closed symbols adsorption; open symbols desorption.

4. CONCLUSIONS

A change in the identity of the synthesis solvent, together with postpolymerization thermal treatment, results in a doubling of the nitrogen-accessible surface area of the previously described POP material, **YSN-1**. The enhancements appear to derive from a decrease in catenation (solvent induced) and from conversion of mesopores to micropores (thermally induced), ultimately yielding a POP with a surface area of ca. 2,500 m^2/g. It would be interesting to see to what extent the thermal enhance behavior is generalizable. The best candidates are likely to be ones that show significant, unexpected mesoporosity together with expected microporosity in experimental plots of pore size distribution.[8d]

A new, but related, material, **YSN-2**, displays a surface area of ca. 2,000 m^2/g. While far from record-high values, the surface areas of **YSN-1** and **YSN-2**, place them among the half dozen or so, highest SA POPs to date. Both materials display excellent thermal and chemical stability, consistent with their assembly via formation of strong carbon−carbon bonds. An exploratory assessment of cryogenic adsorption of molecular hydrogen by **YSN-1** yielded a maximum uptake (excess sorption) of 3.7 wt % at ca. 17 bar. This value is broadly consistent with expectations based on **YSN-1**'s surface area relative to other microporous materials.[7]

■ ASSOCIATED CONTENT

ⓢ Supporting Information

Additional gas isotherm data, FTIR data, and procedure details. This material is available free of charge via the Internet at http://pubs.acs.org.

■ AUTHOR INFORMATION

Corresponding Author
*E-mail: o-farha@northwestern.edu (O.K.F.), j-hupp@northwestern.edu (J.T.H.).

Author Contributions
‡These authors contributed equally.

Notes
The authors declare no competing financial interest.

■ REFERENCES

(1) (a) Lee, J.; Farha, O. K.; Roberts, J.; Scheidt, K. A.; Nguyen, S. T.; Hupp, J. T. *Chem. Soc. Rev.* **2009**, *38*, 1450−1459. (b) Kaur, P.; Hupp, J. T.; Nguyen, S. T. *ACS Catal.* **2011**, *1*, 819−835. (c) Ma, L.; Abney, C.; Lin, W. *Chem. Soc. Rev.* **2009**, *38*, 1248.

(2) (a) Murray, L. J.; Dincă, M.; Long, J. R. *Chem. Soc. Rev.* **2009**, *38*, 1294. (b) Hu, Y. H.; Zhang, L. *Adv. Mater.* **2010**, *22*, E117.

(3) (a) Li, J.-R.; Kuppler, R. J.; Zhou, H.-C. *Chem. Soc. Rev.* **2009**, *38*, 1477. (b) An, J.; Geib, S. J.; Rosi, N. L. *J. Am. Chem. Soc.* **2010**, *132*, 38. (c) Bae, Y.-S.; Farha, O. K.; Hupp, J. T.; Snurr, R. Q. *J. Mater. Chem.* **2009**, *19*, 2131. (d) Britt, D.; Furukawa, H.; Wang, B.; Glover, T. G.; Yaghi, O. M. *Proc. Natl. Acad. Sci. U. S. A.* **2009**, *106*, 20637.

(4) Weitkamp, J.; Fritz, M.; Ernst, S. *Int. J. Hydrogen Energy* **1995**, *20*, 967−970.

(5) Tranchemontagne, D. J.; Mendoza-Cortes, J. L.; O'Keeffe, M.; Yaghi, O. M. *Chem. Soc. Rev.* **2009**, *38*, 1257−1283.

(6) (a) Cote, A. P.; Benin, A. I.; Ockwig, N. W.; O'Keeffe, M.; Matzger, A. J.; Yaghi, O. M. *Science* **2005**, *310*, 1166−1170. (b) Hunt, J. R.; Doonan, C. J.; LeVangie, J. D.; Cote, A. P.; Yaghi, O. M. *J. Am. Chem. Soc.* **2008**, *130*, 11872−11873.

(7) (a) Dawson, R.; Cooper, A. I.; Adams, D. J. *Prog. Polym. Sci.* **2012**, *37*, 530−563. (b) McKeown, N. B.; Budd, P. M. *Macromolecules* **2010**, *43*, 5163−5176.

(8) (a) Farha, O. K.; Spokoyny, A. M.; Hauser, B. G.; Bae, Y.-S.; Brown, S. E.; Snurr, R. Q.; Mirkin, C. A.; Hupp, J. T. *Chem. Mater.* **2009**, *21*, 3033−3035. (b) Farha, O. K.; Bae, Y.-S.; Hauser, B. G.; Spokoyny, A. M.; Snurr, R. Q.; Mirkin, C. A.; Hupp, J. T. *Chem. Commun.* **2010**, *46*, 1056−8. (c) Dawson, R.; Stockel, E.; Holst, J. R.; Adams, D. J.; Cooper, A. I. *Energy Environ. Sci.* **2011**, *4*, 4239−4245. (d) Kassab, R. M.; Jackson, K. T.; El-Kadri, O. M.; El-Kaderi, H. M. *Res. Chem. Intermed.* **2011**, *37*, 747−757.

(9) (a) Saha, D.; Deng, S. *J. Phys. Chem. Lett.* **2009**, *1*, 73−78. (b) Zhou, W.; Wu, H.; Yildirim, T. *Chem. Phys. Lett.* **2010**, *499*, 103−107.

(10) Weber, J.; Schmidt, J.; Thomas, A.; Bohlmann, W. *Langmuir* **2010**, *26*, 15650−15656.

(11) Xie, L.-H.; Liang, J.; Song, J.; Yin, C.-R.; Huang, W. *Curr. Org. Chem* **2010**, *14*, 2169−2195.

(12) Schmidt, J.; Werner, M.; Thomas, A. *Macromolecules* **2009**, *42*, 4426−4429.

(13) Ben, T.; Ren, H.; Ma, S.; Cao, D.; Lan, J.; Jing, X.; Wang, W.; Xu, J.; Deng, F.; Simmons, J. M.; Qiu, S.; Zhu, G. *Angew. Chem., Int. Ed.* **2009**, *48*, 9457−9460.

(14) Yuan, D.; Lu, W.; Zhao, D.; Zhou, H.-C. *Adv. Mater.* **2011**, *23*, 3723−3725.

(15) Walton, K. S.; Snurr, R. Q. *J. Am. Chem. Soc.* **2007**, *129*, 8552−8556.

(16) (a) Weber, J.; Antonietti, M.; Thomas, A. *Macromolecules* **2008**, *41*, 2880−2885. (b) Schmidt, J.; Weber, J.; Epping, J. D.; Antonietti, M.; Thomas, A. *Adv. Mater.* **2009**, *21*, 702−705. (c) Yuan, S.; Kirklin, S.; Dorney, B.; Liu, D.-J.; Yu, L. *Macromolecules* **2009**, *42*, 1554−1559.

(17) Dawson, R.; Laybourn, A.; Khimyak, Y. Z.; Adams, D. J.; Cooper, A. I. *Macromolecules* **2010**, *43*, 8524−8530.